CHEMISTRY
A EUROPEAN JOURNAL

Car–Parrinello Molecular Dynamics Study of the Initial Dinitrogen Reduction Step in Sellmann-Type Nitrogenase Model Complexes

Barbara Kirchner,*[a] Markus Reiher,[a] Andreas Hille,[b, d] Jürg Hutter,[c] and Bernd A. Hess[a]

In memory of Professor Dieter Sellmann

Abstract: We have studied reduction reactions for nitrogen fixation at Sellmann-type model complexes with Car–Parrinello simulation techniques. These dinuclear complexes are especially designed to emulate the so-called open-side FeMoco model. The main result of this work shows that in order to obtain the reduced species several side reactions have to be suppressed. These involve partial dissociation of the chelate ligands and hydrogen atom transfer to the metal center. Working at low temperature turns out to be one necessary pre-requisite in carrying out successful events. The successful events cannot be described by simple reaction coordinates. Complicated processes are involved during the initiation of the reaction. Our theoretical study emphasizes two experimental strategies which are likely to inhibit the side reactions. Clamping of the two metal fragments by a chelating phosphane ligand should prevent dissociation of the complex. Furthermore, introduction of *tert*-butyl substituents could improve the solubility and should thus allow usage of a wider range of (mild) acids, reductants, and reaction conditions.

Keywords: density functional calculations · iron · molecular dynamics · nitrogen fixation · sulfur

Introduction

Biological nitrogen fixation is supposed to take place at the FeMo cofactor (FeMoco) which is the active center of the enzyme nitrogenase.[1,2] The core of this transition metal sulfur cluster consists of seven iron and one molybdenum metal atoms. Several density functional theory (DFT) studies on FeMoco were published thus far.[3–7] Although they do not agree in essential steps of the biological mechanism, they all suggest that the reduction reaction starts at the iron centers of FeMoco. Recently, the first nitrogen reducing complex that works catalytically at the ambient conditions of nitrogenase was synthesized.[8] It consists of a single molybdenum atom in a triamido-amine chelate ligand environment. Attempts to accomplish catalytic dinitrogen reduction at metal centers with a sulfur atom environment were unsuccessful so far.

About a decade ago Sellmann suggested the so-called open-side FeMoco model. He postulated that FeMoco opens in order to bind dinitrogen at the iron-metal centers.[9] This model was substantiated by some of the above-mentioned DFT calculations only recently.[6,7] A main goal of Sellmann and co-workers was the synthesis of a sulfur-based dinitrogen-reducing ruthenium or iron complex with the properties of working i) catalytically, ii) at ambient conditions and iii) by using only moderately strong reductants.[10,11] To date, $[\mu\text{-}N_2\{Ru(P\mathit{i}Pr_3)(\text{“}N_2Me_2S_2\text{”})\}_2]$[“$N_2Me_2S_2$”$^{2-}$ = 1,2-ethanediamine-*N*,*N*′-dimethyl-*N*,*N*′-bis(2-benzenethiolate)(2−)], represents the only known example of a stable dinuclear metal–sulfur N_2 complex.[12,13] After its synthesis in 2001, extensive experimental research was carried out in order to determine

[a] Dr. B. Kirchner, Priv.-Doz. Dr. M. Reiher, Prof. Dr. B. A. Hess
Lehrstuhl für Theoretische Chemie, Universität Bonn
Wegelerstrasse 12, 53115 Bonn (Germany)
Fax: (+49) 228-73-9064
E-mail: kirchner@thch.uni-bonn.de

[b] Dr. A. Hille
Lehrstuhl für Anorganische Chemie
Universität Erlangen-Nürnberg, Egerlandstrasse 1
91058 Erlangen (Germany)

[c] Prof. Dr. J. Hutter
Physikalisch-chemisches Institut, University at Zürich
Winterthurerstrasse 190, 8057 Zürich (Switzerland)

[d] Dr. A. Hille
present address:
Department of Chemistry, Cambridge University, Lensfield Road
Cambridge CB2 1EW (England)

DOI: 10.1002/chem.200400709

whether this dinuclear N_2 complex can be reduced to give the corresponding diazene complex [μ-N_2H_2{Ru-($P\mathit{i}Pr_3$)("$N_2Me_2S_2$")}$_2$]. This compound, which was obtained previously by a separate synthesis, has been fully characterized and is reported elsewhere in detail.[14] Until now the full catalytic cycle could not be established. Already the crucial first endothermic reduction step turns out to be difficult to achieve.[15] Instead of reduction to diazene various side reactions were detected during the experiments.

According to Figure 1, several reaction pathways were experimentally tested to reduce the N_2 complex. However, these first experiments have not yet yielded an indication that a dicationic diazene species can be trapped by adding protons to solutions of the N_2 complex while irradiating these solutions with UV light ($\upsilon = 314$ nm) along path 1 in Figure 1. Also, first experimental reduction experiments were not successful with respect to the direct reduction of the N_2 ligand in the complex (path 3, Figure 1). Apparently, protonation (path 2) of the sulfur donors should be considered as an essential and most promising initial step during the reduction of the dinuclear N_2 complex.[9,10,16–29]

It is the purpose of this study to investigate this first protonation reduction step in order to obtain a microscopic picture of a possible mechanism of a two-electron reduction of protonated Sellmann-type complexes. A detailed understanding of the reaction mechanism should yield suggestions for a particular ligand sphere for sulfur-rich metal complexes designed to stimulate nitrogen activation. We considered two complexes: a small [Ru"S_2N_2"]$_2$L model complex and a larger [Fe"N_HS_4"]$_2$L complex (see Figure 2).

For both of complexes we observed[30] a characteristic bending of the linear N_2 moiety towards an activated diazenoid structure upon either photochemical activation or reduction. Additionally, we chose these two particular examples out of the variety of Sellmann-type Fe^{II}- and Ru^{II}–sulfur complexes[9–11,28,31] for two reasons: i) as already mentioned the first dinitrogen metal–sulfur complex was experimentally found for a similar (albeit significantly larger) Ru"S_2N_2" system[13,14,32] and ii) our aim is the investigation of complexes with chelate ligands of different rigidity in

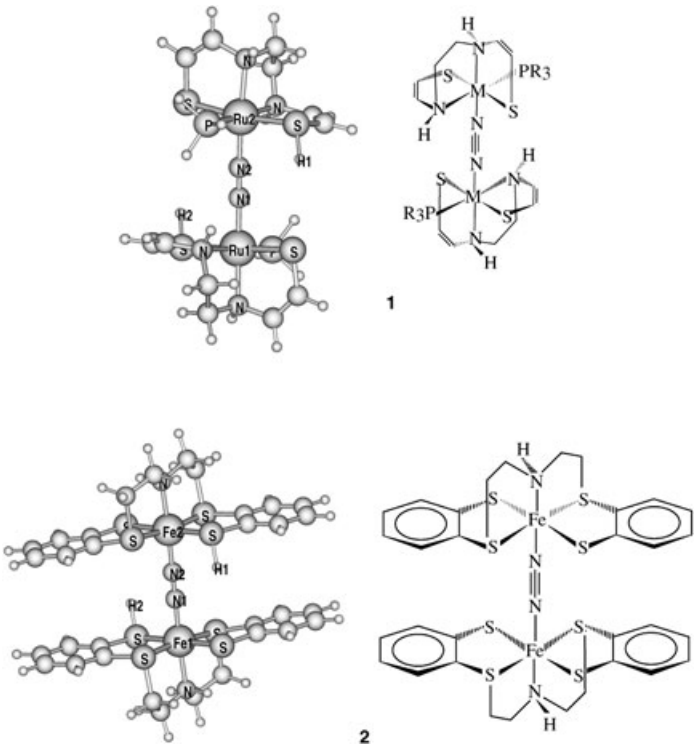

Figure 2. Sellmann-type Ru"S_2N_2" model complex **1**N_2 (top) and Fe"N_HS_4" complex **2**N_2 (bottom) investigated in this work.

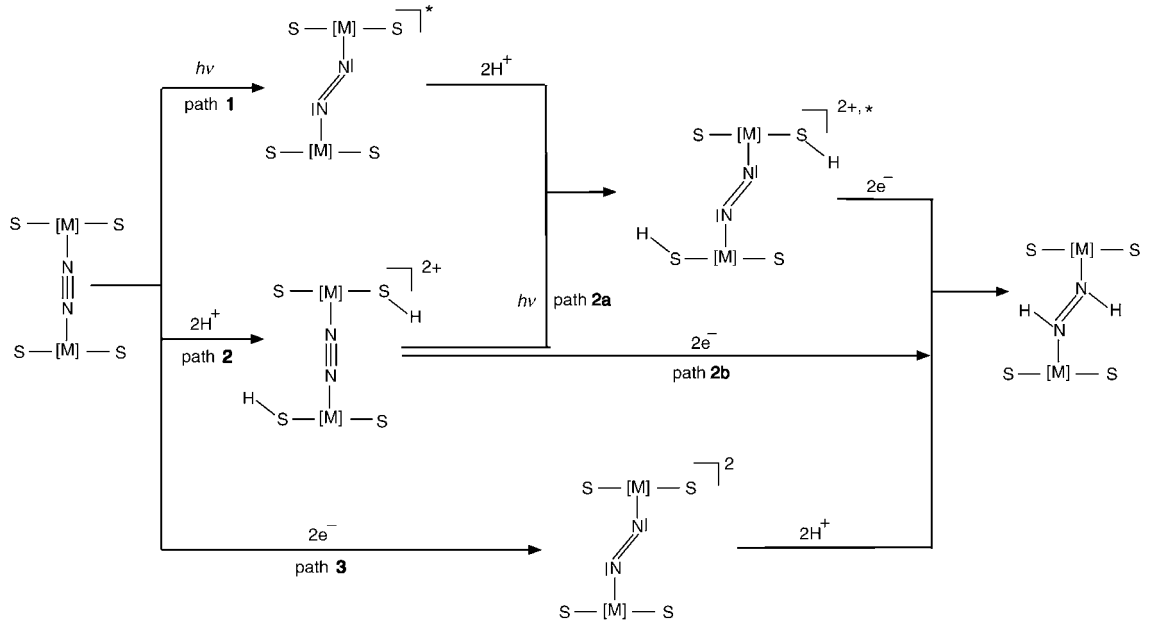

Figure 1. Possible paths of reducing the dinitrogen model complex assuming a *cis*-symmetrically diprotonated start species or intermediates.

order to elucidate the general properties of Sellmann-type complexes. Therefore, we also investigated the Fe"N_HS_4"-based complexes, of which the diazene complex (i.e., the product of the reduction reaction) exists in synthesis.[33]

Since we are interested in a detailed time-resolved picture of the process, we carried out Car–Parrinello simulations of the reaction steps (see Figure 1, especially path 2b) of the electron-coupled proton transfer. The Car–Parrinello simulation technique is especially suitable for this purpose as it is able to adjust spontaneously to different molecular binding scenarios while at the same time it also describes the time evolution of the system by molecular dynamics simulation. Three situations are possible in a molecular dynamics simulation: i) starting at a local maximum or mechanistically well-defined high-energy non-stationary structure in order to provide a starting point for relaxations into a valley or ii) starting at a structure below a barrier, which is so small ($\Delta G^{\neq} < kT$) that the reaction actually does occur, or iii) employing constraints along a possibly good reaction coordinate and forcing the reaction to occur. The latter technique would allow us to calculate a free energy ΔG and $\Delta G^{\neq}$ if the transition state is located by integrating the constraint force. At each constraint value the sampling introduces a considerable arbitrariness. If the simulation is started close to a transition state to run down a hill, we should in principle also be able to start from many slightly different situations in order to obtain a statistically averaged thus unbiased situation and thus an average passage time for the down-hill process. However, following only a single trajectory down-hill yields a time for this process; its order of magnitude might be considered as a first hint, and a possible reaction mechanism.

Starting point for this investigation were the photo-activation reactions proposed earlier[30] and the observation that geometry optimization of protonated doubly reduced (i.e., uncharged) Sellmann-type complexes (path 2b) directly leads to a hydrogen transfer from the sulfur donors of the chelate ligand sphere onto the dinitrogen ligand.[38] The key step in these processes is the occupation of the LUMO (either by reduction or by photo-activation), which exhibits a pronounced antibonding character at the N_2 ligand and thus allows bending of the linear [M]-N≡N-[M] unit yielding an activated diazenoid N_2 species ready for proton uptake.

Theoretical Methodology

For the Car–Parrinello molecular dynamics simulations we used the CPMD code[34] employing Troullier Martins norm-conserving pseudo potentials[35] with a 70 Ryd cut-off. For all atoms excluding ruthenium and iron we chose the electron configuration of the neutral atomic ground state. Ruthenium was treated as an ionic system in the Ru^{2+} configuration and iron in the Fe^{2+}, that is, electron configuration $4d^6$ and $3d^6$ and in an oxidation state of +II. The 4s and 4p semi-core states were included explicitly in the calculation. The core radii (r_c in atomic units) were 1.2 for carbon, 1.12 for nitrogen, 1.5 for phosphorus, 1.4 for sulfur, and 0.5 for hydrogen. The same values for all angular momentum states were employed. The r_c values for ruthenium were 1.1 (L=0), 1.2 (L=1) and 1.6 for (L=2). For iron it was 1.9 (L=0), 2.0 (L=1) and 1.5 for (L=2) and 1.97 (L=3). Hydrogen was described by a local pseudopotential. For nitrogen and carbon s and p, for sulfur, phosphorus, ruthenium and iron s, p, and d angular momentum functions were included. The highest angular momentum channels were used as local potentials. For iron we applied the non-linear core correction. In general integration was carried out with the Kleinman–Bylander[36] scheme, except in the case of ruthenium and iron atoms where a Gauss–Hermite integration scheme with 20 integration points was applied. The electronic structure was described by using the BP86 density functional. To enable the study of isolated systems, the inherent periodicity in the plane-wave calculations was avoided by solving Poisson's equation with non-periodic boundary conditions.[37] To optimize the wavefunction we employed the "preconditioned conjugate gradients" method with convergence criteria of 10^{-6} and 10^{-3} for the largest element of the gradient of the wavefunction and for the ions, respectively. The cell size was set to $20\times20\times20$ Å^3, which was sufficient to converge the energies and geometries with respect to the cell parameters. The initial experiment time step was set to 3 au and the fictitious electron mass to 400 au. After several tests we increased the time step to 5 au and the fictitious electron mass to 600 au in order to save computer time.

Results

Reaction coordinate and possible mechanisms

The following paragraphs describe a sequence of constrained and free simulations of both complexes **1**N_2 and **2**N_2 at different temperatures. The simulation experiments are constructed as visualized schematically in Figure 3: Two protons are bound to the system **A**, and a two-electron reduction leads to a complex B1 on the corresponding electronic energy surface on which the simulation takes place to end in structure **C**.

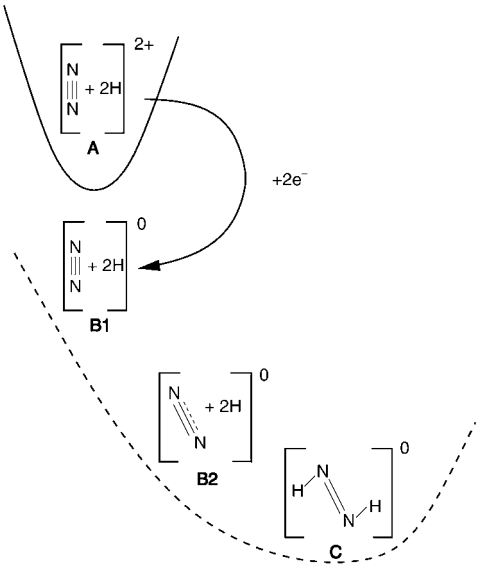

Figure 3. Schematic drawing of initial state preparation.

We set up different initial situations of the complexes by starting from:

A: the optimized two-fold positively charged complex **1** of ref. [30]

B1: two electrons added to **A**, making it a neutral complex

C: the optimized structure of **B1** from ref. [30]

B2: a structure which is obtained by stopping the preparation of **C** during the course of the reaction

Since structures **B1** and **B2** are high-energy structures on the potential energy surface of the neutral species, we are able to observe spontaneous events (note that this exactly reflects the desired picture, which emerges after fast electron transfer onto the diprotonated complex). Because of the very computer-time consuming CPMD calculations no extended statistics are available. However, the simulations still point to a potential mechanism and a possible reaction coordinate by observing how the prepared states **B1** or **B2** behave under temperature, forced bending, and forced decrease of the nitrogen proton distances. In the following we will always start from configuration **B1** of the complex $\mathbf{2}N_2$ unless otherwise stated.

Side reactions

Dissociation of the chelate ligand: It is most intuitive to enforce a possible event by applying a nonzero temperature. For approximately 350 fs we carried out a free molecular dynamics simulation thermostated at 320 K (average $T=$ 301 K) by using complex $\mathbf{2}N_2$. We observed a partial dissociation of the chelate ligands and the hydrogen atoms move away from the nitrogen atoms instead of approaching them (see Figure 4). The mechanism leading to this increased N···H distance is governed by the increase of the FeSH angle from 100 to 117° for the H1 and from 100 to 172° for the H2 atom. The corresponding S–H distances are not disturbed; they only change their values due to vibrational motion in the range of 20 pm.

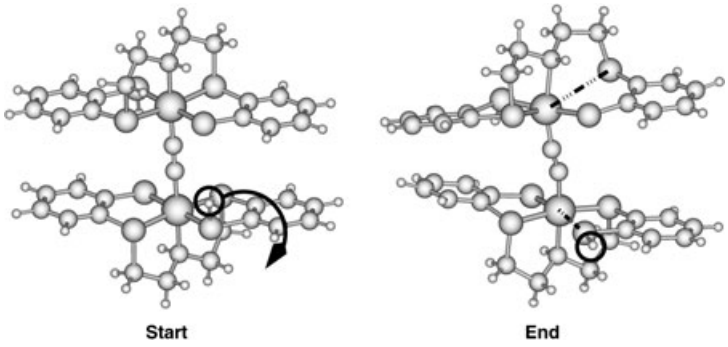

Figure 4. Sketch of the hydrogen atom dynamics away from the reaction center and observed partial dissociation of the chelate ligand in complex $\mathbf{2}N_2$.

In order to see whether the dissociation is a result of the hydrogen atom which approaches the chelate ligand instead of the dinitrogen moiety and whether one hydrogen atom aims into the right direction if the other one is forced to stay close to the corresponding nitrogen atom (i.e., the one it is supposed to react with), we started a simulation prepared as described before, though one hydrogen–nitrogen distance was kept fixed. After 232 fs once more a dissociation in parts of the chelate ligands at both metal centers was observed in the same manner as before.

In a next step, we fixed all six inner shell chelate ligand atoms bound to the metal center. As a result the chelate ligands were not allowed to dissociate. Still the hydrogen atoms do not approach the dinitrogen—but rather increase the N···H distance in oscillating motion by enlargement of the MSH angle. The same was observed if all six inner shell chelate ligands were fixed to the metal centers including the dinitrogen.

Hydrogen transfer to the metal center: We observed another side reaction at the $\mathbf{2}N_2$ model complex by decreasing one N···H distance by using a constraint algorithm which allows the particular distance only to become smaller but not to grow above the achieved value again. The other hydrogen atom was allowed to evolve freely without applying constraints. The temperature was again kept at 320 K with Nose–Hoover thermostats leading to an average temperature of 315 K.

In Figure 5 the result of this constraint simulation is shown. Whereas the free hydrogen atom still leaves the proximity of the N_2 moiety and the chelate ligand (partially) dissociates, the constraint N···H distance does indeed decrease, but the hydrogen atom is transferred to the metal center instead of the nitrogen atom. Subsequent to this simulation, we allowed the system to evolve without any constraint to see whether the hydrogenated metal fragment dissociates from the rest of the complex or whether the free hydrogen atom changes the direction of its motion. The tendency of the hydrogen atom which was not transferred is to be further away from the nitrogen atom whereas the nitrogen nitrogen distance becomes slightly smaller. However, nothing noteworthy happens on the time scale we were able to simulate. The same results were obtained in the case where both hydrogen nitrogen distances are forced to decrease at 320 K.

Successful events

Because it could be shown before[30] that the bending of the nitrogen moiety is an important step, we forced both hydrogen MNN angles to decrease in time in complex $\mathbf{2}N_2$ with an algorithm that allows these angles only to become smaller or to keep their current value but not to grow above that current value again.

The larger time step was applied for this experiment. Interestingly, the molecule keeps its symmetry during the time evolution. This is the reason why we only show one curve in each panel of Figure 6. After the first run the temperature is lowered from 320 to 100 K to avoid the dissociation of the chelate ligands. The reaction starts—as can be seen in Figure 6—at 600 fs involving a sequence of complicated processes.

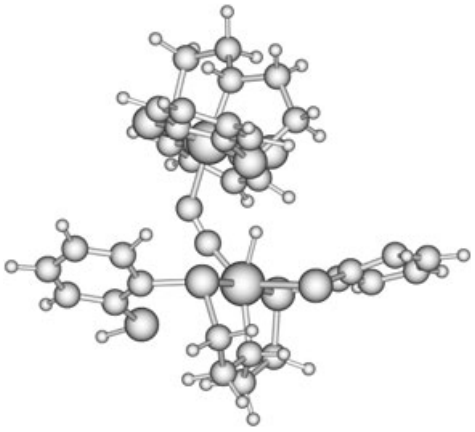

Figure 5. Resulting structure of the algorithm applied to decrease one hydrogen–nitrogen distance in complex **2**N_2.

We observe an increase of the Kohn–Sham energy and temperature indicating a small barrier at an initial time step of 150 fs depicted in Figure 7. This barrier is related to

1) a slight increase (5 pm) of the N–N distance, see panel 1, Figure 6,
2) an increase (150 pm) of the hydrogen nitrogen atom distance in analogy to the first side reaction, see panel 2 Figure 6,
3) an elongation (15 pm) of the metal nitrogen distance and to an enlargement of the FeSH angle (20°), see panels 5 and 6 of Figure 6.

This shows that in the starting configuration **B1** (Figure 3) the bending of the N_2 moiety is structurally hindered. A smaller barrier of about 0.025 au is indicated by the increase

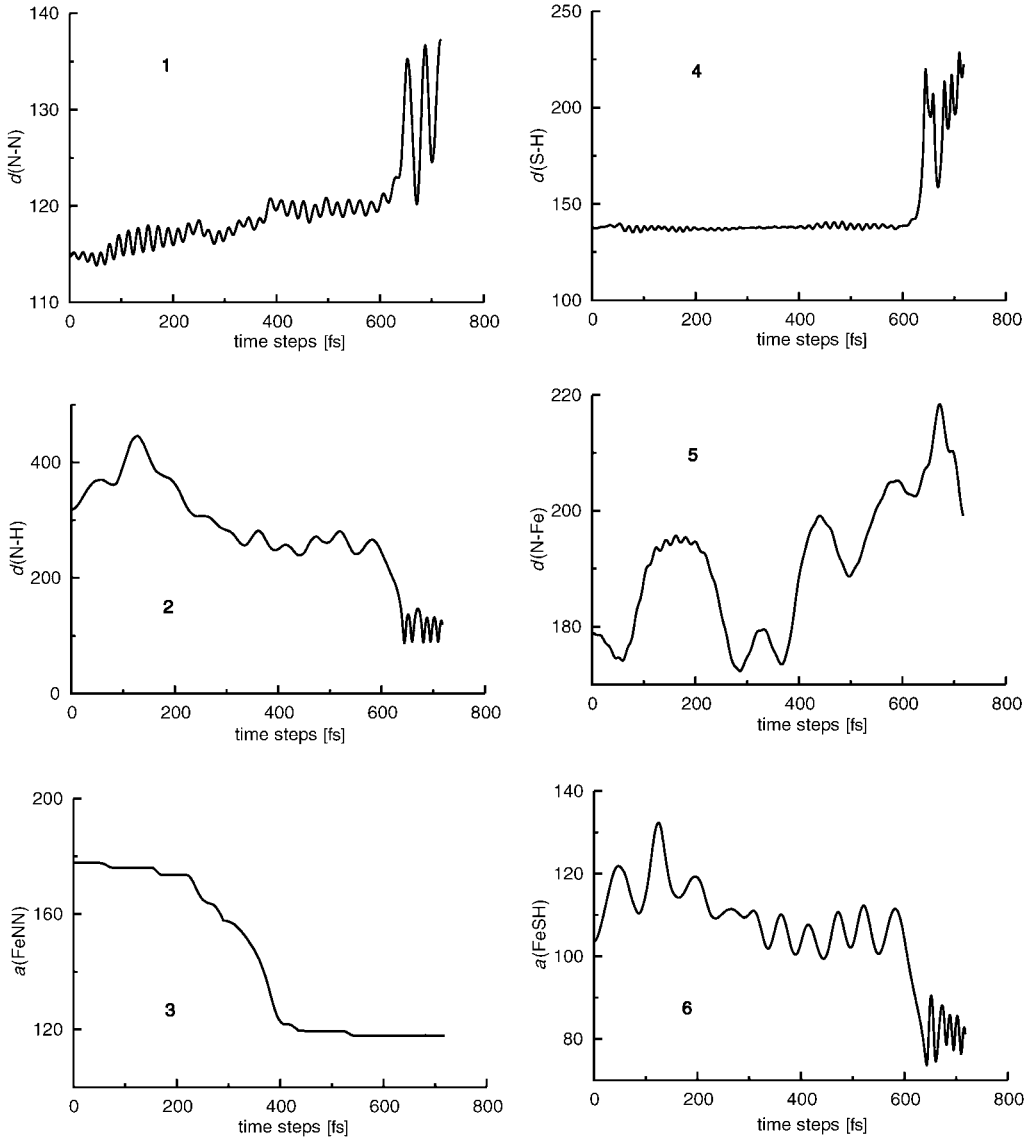

Figure 6. Results of the simulation of the large Fe complex **2**N_2 where the MNN angles are forced to decrease with time. 1) Nitrogen–nitrogen distance, 2) nitrogen–hydrogen distance, 3) MNN angle, 4) sulphur–hydrogen distance, 5) N–M distance, 6) MSH angle; distances in pm, angles in degrees.

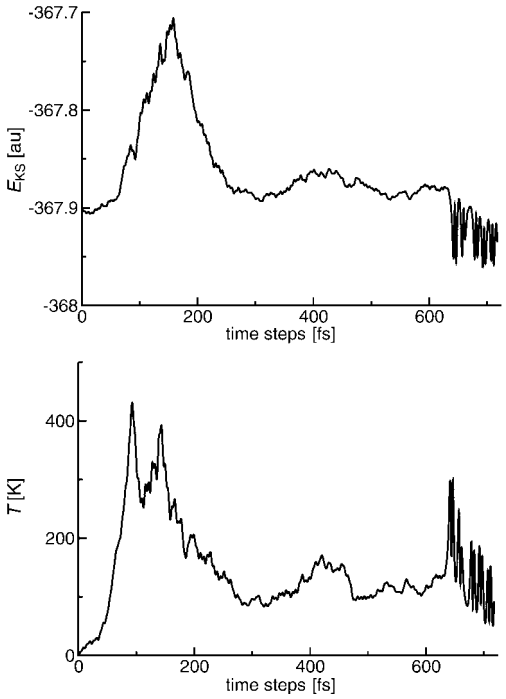

Figure 7. Results of the algorithm applied to decrease both metal-nitrogen-nitrogen angles. Top: Kohn–Sham energy plotted against time steps, bottom: temperature evolution with time steps.

of the Kohn–Sham energy at a time step of about 300 fs, where the bending of the FeNN angle is initiated as shown in panel 3. When the actual reaction takes place at 600 fs the Kohn–Sham energy drops down and the temperature is heated up by 150 K. The observation of the reaction under these special constraint forces seems to indicate that for the reaction to occur it is necessary to bend the M1N1N2 and M2N2N1 angles. Unless the hydrogen atoms leave the proximity of the nitrogen atoms it appears that this bending of the N_2 moiety is prohibited. It should be noted that both hydrogen atoms are transferred simultaneously. We tested whether only one angle constraint would lead to a non-simultaneous reaction. This was not the case, the process also occurred simultaneously.

A more natural situation is modeled in a free simulation which we carried out for both Sellmann models $\mathbf{1}N_2$ and $\mathbf{2}N_2$.

Figure 8 shows the simulation results of the small Sellmann model $\mathbf{1}N_2$ without applying constraints at 50 K. This simulation is started from a pre-bent structure (**B2** of Figure 3). After approximately 450 fs the N_2 moiety starts to react with one hydrogen atom (H2–N2). In this experiment the transfer of the two hydrogen atoms does not occur simultaneously. As before several features can be observed how the reaction takes place, see Figure 8. The dinitrogen bond vibrates and the bond length increases in the course of the 450 fs, see panel 1 in Figure 8. Vibrations with a small amplitude around an average distance of 121.5 pm indicate the original triple bond before further bending occurs. After the reaction large amplitude vibrations around an average distance of 129.2 pm show the formation of a double bond. Vibrational motion is also observed for the hydrogen–nitrogen bonds, see panel 2. In addition, one NH distance (see dashed curve) is increased in the beginning to allow the other hydrogen atom to approach its nitrogen atom. The reaction for the hydrogen atom with initially increased bond length is delayed. The vibrational motion of both distances

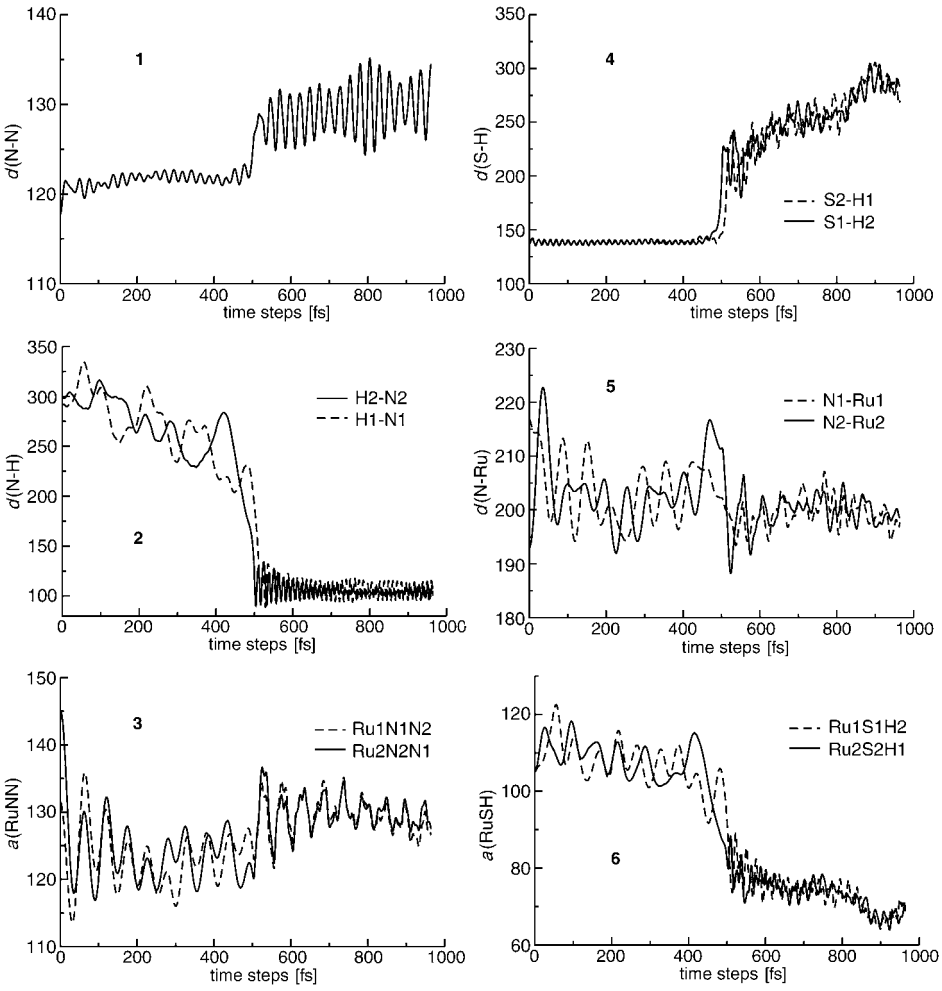

Figure 8. Results of the free simulation of the bent small Sellmann-type complex $\mathbf{1}N_2$. 1) Nitrogen–nitrogen distance, 2) nitrogen–hydrogen distances, 3) RuNN angles, 4) sulphur–hydrogen distances, 5) nitrogen–Ru distances, 6) RuSH angles; distances in pm, angles in degrees.

is anticorrelated. An oscillating motion of the hydrogen atoms leads to their appearance at the nitrogen atoms until at approximately 450 fs where the curve of one distance drops downwards rapidly. This shows that a distance as well as an angle constraint would be an inappropriate reaction coordinate, because the reaction is coupled to more than one simple geometry reaction coordinate. The corresponding RuNN angle has now its smallest maximum and the first hydrogen atom transfer occurs. After only 15 fs the second hydrogen atom is transferred. In panel 3 we see that whereas initially the RuNN angles display pseudo-harmonic vibrational motions, they vibrate afterwards more abruptly and not with such a large amplitude as before. Especially small values of the angles are prohibited by presence of the hydrogen atoms.

The initiation of the reaction is also reflected in panels 4–6 of Figure 8. In panel 4 the S–H distances abruptly grow at 450 fs and vibrate with larger amplitude: the bond is broken. The N–Ru distances do not change much upon reaction but they vibrate with smaller amplitude after the hydrogen-atom transfer (panel 5). The RuSH angles are plotted in panel 6 of Figure 8 and again indicate the change of the S–H bonding situation: they are restricted to values below 90°.

Again the Kohn–Sham energy and the temperature are very close indicators for the course of the reaction (see Figure 9). The Kohn–Sham energy drops noticeably when the H atom is transferred and the system heats up by 100 K.

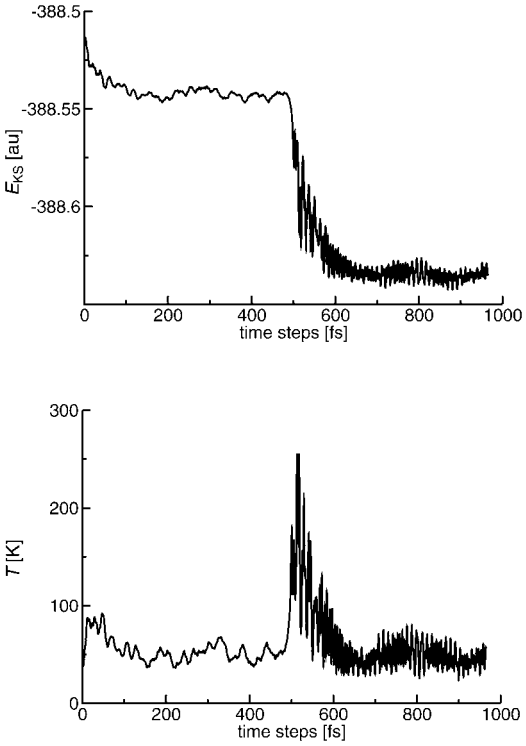

Figure 9. Energy and temperature of the free simulation of the bent ruthenium model complex **1**. Top: Kohn–Sham energy, bottom: temperature; all windows against the time steps.

Encouraged by these results we also carried out a simulation without constraints at 100 K for the Fe complex $\mathbf{2}N_2$ (see Figures 10 and 11).

Again we observe features that this event has in common with the successful events described above for complex $\mathbf{1}N_2$. Before bending of the FeNN angles can occur (panel 3, Figure 10), the hydrogen atom has to move away from the corresponding nitrogen atom. After the initiation the vibrational motion of the latter angles is almost as smooth as in the event of the bent $\mathbf{1}N_2$ model. When the transfer starts at 1050 fs suddenly the changes in both FeNN angles take place more abruptly and in a correlated manner, see panel 3. The S–H distance is never distorted (panel 4, Figure 10), that is, we never see a bond elongation or a shortening exceeding the usual vibrational motion. Only when the H-atom transfer starts the bonds are elongated and thus break. The 20 pm increase of the N–Fe distance (panel 5, Figure 10) occurs only at the side where the reaction starts (see dashed curve); this indicates that the N2–Fe1 distance. Panel 6 shows the MSH angles, which increase at the beginning of the experiment, and only this controls the departure of the H from the nitrogen moiety.

From the three successful reaction events we deduce that the bending motion of the MSH angle is very important for the reaction to take place, because it controls an increase of the N···H distance (panel 2, Figure 10), which again allows the bending motion of the MNN angle to start (panel 3). Even for the pre-bent structure the hydrogen–nitrogen distance has to increase to allow the MNN angles further to exercise their bending mode. This again is a crucial step for the reaction to take place. The S–H distance (panel 4) is never distorted until the transfer takes place, that is, there is no stretching mode involved but a bending mode in the transfer reaction.

The most important difference between the angle-constraint experiment and the free simulations is that in the former the reaction occurs simultaneously whereas in the free simulations the transfer is stepwise. The artificial effect of the constraint applied is reflected in the fact that the MNN angles (panel 3) of Figure 6 move unphysically without vibrational motion.

The main difference between the two unconstraint simulations is that in the first case the simulation starts from a pre-bent **B2** and in the other case from the linear **B1** model. Moreover, the complexes ($\mathbf{1}N_2$ and $\mathbf{2}N_2$) possess different chelate ligands and we carry out the simulations at different temperature (50 and 100 K). This is reflected in the two processes. In panel 1 of Figure 8, we see that the slight increase in the N–N distance does not occur for $\mathbf{1}N_2$ model, because we already start at a pre-bent structure simulation. In panel 3 of Figure 10 the pre-bending becomes apparent, because the MNN angle vibrates only around 10° in the linear configuration for 200 fs and then decreases to 160°, never growing above this value again. Whereas the M N distances in the bent $\mathbf{1}N_2$ model are stretched by about the same values, the equivalent distances for the linear $\mathbf{2}N_2$ are stretched by different values compared to each other: The

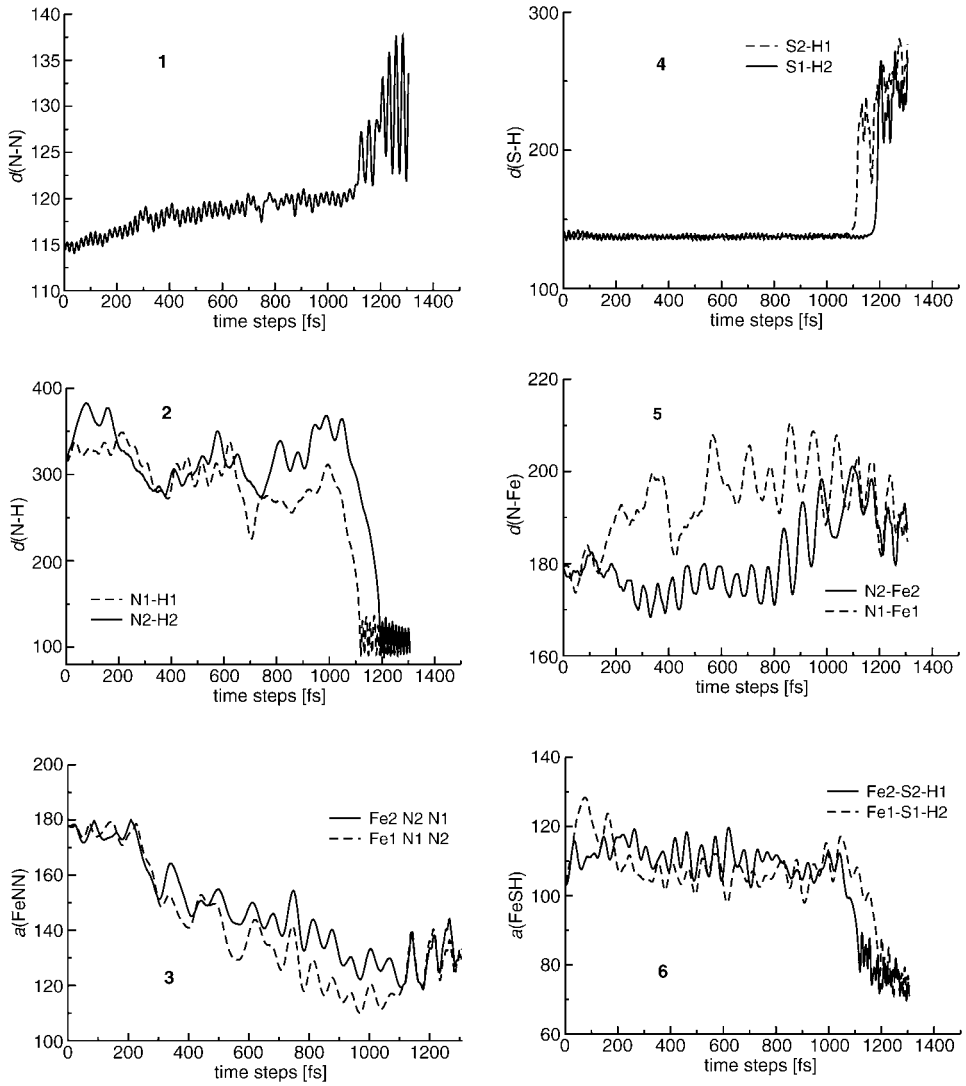

Figure 10. Free simulation results of the large Fe complex $\mathbf{2}N_2$ at 100 K. 1) Nitrogen–nitrogen distance, 2) nitrogen–hydrogen distances, 3) FeNN angles, 4) sulphur–hydrogen distances, 5) nitrogen–Fe distances, 6) FeSH angles; distances in pm, angles in degrees.

distance is stretched more in the case of the side where the reaction occurs first, see dashed graph panel 5 Figure 10. Nevertheless, both instances exhibit quite similar patterns.

Experimental Point of View and Discussion

The mandatory initial protonation of Sellmann-type complexes such as $[\mu\text{-}N_2\{Ru(P\textit{i}Pr_3)(\text{“}N_2Me_2S_2\text{”})\}_2]$ (the parent system of model $\mathbf{1}N_2$) faces fundamental problems. For instance an optimization of the chelate ligand is required: It either decomposes or it is not soluble in most common solvents. In solvents that stabilize the complex, it is only moderately soluble (which does not favor low-temperature experiments suggested by the calculations). Moreover, it partially dissociates in solution to give the coordinatively unsaturated $[Ru(P\textit{i}Pr_3)(\text{“}N_2Me_2S_2\text{”})]$ fragment and mononuclear $[Ru(N_2)(P\textit{i}Pr_3)(\text{“}N_2Me_2S_2\text{”})]$ complex. Unfortunately, the comparably weak Brønsted basicity of the thiolate donors necessitates the use of strong acids such as HBF_4 as proton sources and of non- or only weakly basic solvents. Therefore, most of the protonation experiments were carried out in benzene, toluene, and THF.

Although the solubility of $[\mu\text{-}N_2\{Ru(P\textit{i}Pr_3)(\text{“}N_2Me_2S_2\text{”})\}_2]$ is the highest in THF, one has to be aware that protonation of the THF molecule rather than the sulfur donors might also take place. As evidenced by extensive NMR experiments, protonation of the dinuclear N_2 complex to form $[\mu\text{-}N_2H_2\{Ru(P\textit{i}Pr_3)(\text{“}N_2Me_2S_2\text{”})\}_2]^{2+}$ did not occur. However, the formation of a non-classical dihydrogen complex $[Ru(H_2)(P\textit{i}Pr_3)(\text{“}N_2Me_2S_2\text{”})]$ was observed as one product in some of these experiments[38] (see reaction in Figure 12).

It turned out to be difficult to experimentally elucidate the exact mechanism for the formation of this hydrogen complex. In view of the experimental facts, two reaction pathways seem possible: i) Protonation of one (or both) thi-

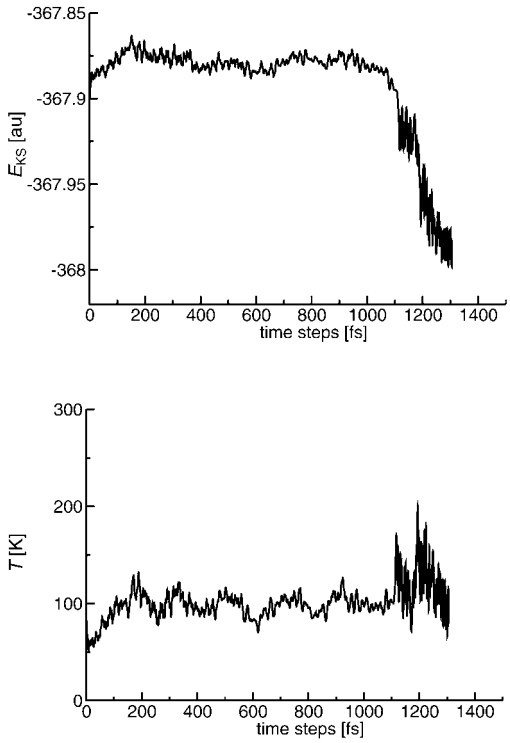

Figure 11. Energy and temperature of the free simulation of the large Fe model complex **2**. Top: Kohn–Sham energy plotted against time steps, bottom: temperature evolution with time steps.

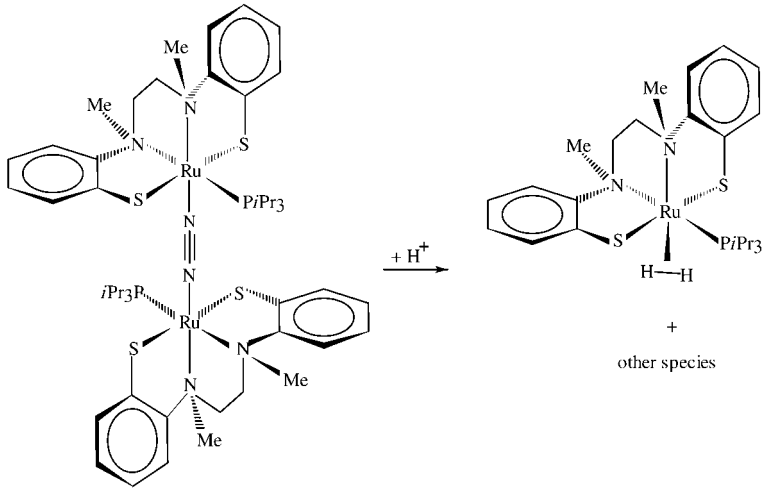

Figure 12. Dissociation reaction of $[\mu\text{-}N_2\{Ru(P\textit{i}Pr_3)(\text{“}N_2Me_2S_2\text{”})\}_2]$ in the presence of acid yields the non-classical dihydrogen complex $[Ru(H_2)(P\textit{i}Pr_3)(\text{“}N_2Me_2S_2\text{”})]$ in experiment (see ref. [38]) which is paralleled by one of the side reactions observed in the CPMD simulations.

olate donors in the dinuclear N_2 complex causes dissociation of the N_2 ligand and formation of an open coordination site (the hydrogen atom is subsequently transferred to this site) or ii) direct reaction of hydrogen atoms occurs with the Ru centers of $[Ru(P\textit{i}Pr_3)(\text{“}N_2Me_2S_2\text{”})]$ fragments, which are always present in solutions of $[\mu\text{-}N_2\{Ru(P\textit{i}Pr_3)(\text{“}N_2Me_2S_2\text{”})\}_2]$ (see above). In both cases, the interaction of hydrogen atoms with the electron rich-metal centers probably results in the evolution of dihydrogen and in the formation of ruthenium(III) and ruthenium(IV) species. This also explains the observation of by-products in the reaction depicted in Figure 12 and nicely agrees the metal-hydrogenation side reaction observed in the CPMD simulation. Note that the hydrogen transfer onto the metal centers was only observed in the simulation if the hydrogen–nitrogen distance was not allowed to increase with the consequence that essential bending of the N_2 moiety is prohibited by structural hindrance.

Summarizing, in order to circumvent experimental problems concerning the protonation of the dinuclear N_2 metal-sulfur complexes as described above, two approaches appear to be promising: i) Introduction of *tert*-butyl substituents at the aromatic rings of the chelate ligand system improves solubility and thus allows one to test a wider range of acids, reductants, and reaction conditions in general and ii) clamping of the two metal fragments by a chelating phosphane ligand of the type $R'_2P\text{-}(CH_2)_n\text{-}PR'_2$ should prevent dissociation of the complex.

Summary and Conclusion

From the CPMD simulations of the initial proton electron transfer step in Sellmann-type nitrogenase model complexes we learn that the initial reduction step is feasible for Sellmann-type complexes if optimal simulation conditions can be met by experiment. The following summarizes results which were observed for both complexes investigated, that is, for $\mathbf{1}N_2$ and for $\mathbf{2}N_2$. The simulations point towards a possible three-step reaction mechanism for the hydrogen atom transfer onto dinitrogen upon reduction: i) Increase of the N···H distance; ii) bending of both MNN angles which yields the activated diazenoid N_2 species, then iii) vibration of the H···N distance which is controlled by the MSH angle and simultaneously vibration of the MNN angles with opposite phase so that the nitrogen atoms can meet the hydrogen atoms.

Moreover, the simulation experiments showed two possible side reactions, which need to be circumvented: i) The movement of the hydrogen atoms away from the nitrogen atoms towards the side of the chelate ligand and ii) the hydrogenation of the metal center. These reactions should be suppressed by suitable ligand design as described at the end of the last section. For a successful reaction to take place the first side reaction, that is, movement of the hydrogen atoms away from the nitrogen atoms, seems to be necessary other-

wise the reaction is structurally hindered. We emphasize that both complexes show equivalent features although the chelate ligands are chemically quite different. We deduce from this that the observed attributes of the nitrogen reduction reaction can be considered universal.

The main result of this work is that Sellmann-type complexes should indeed be able to reduce N_2. Even more important is the fact that the reaction takes place spontaneously if a "*trans*"-diprotonated equilibrium structure of the dinitrogen complex is subjected to a two-electron reduction. From our simulations we can extract a first estimate of the reaction time for a transfer of two hydrogen atoms starting from the "*trans*"-diprotonated dinitrogen complex. The time for this process is of the order of 0.5–1.0 picoseconds. Since fine-tuning of the complex stability (e.g., through a clamping phosphine, *t*Bu substituents at the phenyl rings which increase the solubility and will also reduce the amplitude of motion of the chelate ligand at higher temperature) and of the reaction conditions (temperature, acid, electron donor) is still possible, further experimental investigation of the Sellmann-type complexes is encouraged by the results reported in this work.

Acknowledgement

The authors would like to acknowledge the generous computer time provided by the MPG-RZG Garching and financial support through the collaborative research center SFB 583 "Redoxaktive Metallkomplexe".

[1] O. Einsle, F. A. Tezcan, S. L. A. Andrade, B. Schmid, M. Yoshida, J. B. Howard, D. C. Rees, *Science* **2002**, *297*, 1696–1700.
[2] *Nitrogen Fixation at the Millenium* (Ed.: G. J. Leigh), Elsevier, Amsterdam, **2002**.
[3] B. Hinnemann, J. K. Nørskov, *J. Am. Chem. Soc.* **2004**, *126*, 3920–2937.
[4] B. Hinnemann, J. K. Nørskov, *J. Am. Chem. Soc.* **2003**, *125*, 1466–1467.
[5] I. Dance, *Chem. Commun.* **2003**, 324–325.
[6] J. Schimpl, H. M. Petrilli, P. E. Blöchl, *J. Am. Chem. Soc.* **2003**, *125*, 15772–15778.
[7] U. Huniar, R. Ahlrichs, D. Coucouvanis, *J. Am. Chem. Soc.* **2004**, *126*, 2588–2601.
[8] D. V. Yandulov, R. R. Schrock, *Science* **2003**, *301*, 76–78.
[9] D. Sellmann, J. Sutter, *Acc. Chem. Res.* **1997**, *30*, 460–469.
[10] D. Sellmann, J. Utz, N. Blum, F. W. Heinemann, *Coord. Chem. Rev.* **1999**, *190–192*, 607–627.
[11] D. Sellmann, A. Fürsattel, J. Sutter, *Coord. Chem. Rev.* **2000**, *200–202*, 541–561.
[12] M. Reiher, B. A. Hess, *Adv. Inorg. Chem.* **2004**, *56*, 55–100.
[13] D. Sellmann, A. Hille, F. W. Heinemann, M. Moll, A. Rösler, J. Sutter, G. Brehm, M. Reiher, B. A. Hess, S. Schneider, *Inorg. Chim. Acta* **2003**, *348*, 194–198.
[14] D. Sellmann, A. Hille, A. Rösler, F. W. Heinemann, M. Moll, G. Brehm, S. Schneider, M. Reiher, B. A. Hess, W. Bauer, *Chem. Eur. J.* **2004**, *10*, 819–830.
[15] M. Reiher, B. A. Hess, *Chem. Eur. J.* **2002**, *8*, 5332–5339.
[16] R. H. Holm, P. Kennepohl, E. I. Solomon, *Chem. Rev.* **1996**, *96*, 2239–2314.
[17] R. A. Henderson, *J. Chem. Soc. Dalton Trans.* **1995**, 503–511.
[18] D. Coucouvanis, *Adv. Inorg. Chem.* **1998**, *45*, 1–73.
[19] D. Coucouvanis, K. D. Demadis, S. M. Malinak, P. E. Mosier, M. A. Tyson, L. Laughlin, *ACS Symp. Ser.* **1996**, *653*.
[20] B. E. Smith, *Adv. Inorg. Chem.* **1999**, *47*, 159–218.
[21] M. D. Fryzuk, S. A. Johnson, *Coord. Chem. Rev.* **2000**, *200–202*, 379–409.
[22] A. E. Shilov, *Metal Complexes in Biomimetic Chemical Reactions*, CRC Press, Boca Raton, **1997**.
[23] M. Hidai, Y. Mizobe, *Chem. Rev.* **1995**, *95*, 1115–1133.
[24] M. Hidai, *Coord. Chem. Rev.* **1999**, *185*/186, 99–108.
[25] Y. Nishibayashi, S. Iwai, M. Hidai, *Science* **1998**, *279*, 540–542.
[26] Y. Nishibayashi, S. Takemoto, S. Iwai, M. Hidai, *Inorg. Chem.* **2000**, *39*, 5949–5957.
[27] R. N. F. Thorneley, D. J. Lowe, *J. Biol. Inorg. Chem.* **1996**, *1*, 576–580.
[28] D. Sellmann, J. Sutter, *J. Biol. Inorg. Chem.* **1996**, *1*, 587–593.
[29] D. Coucouvanis, *J. Biol. Inorg. Chem.* **1996**, *1*, 594–600.
[30] M. Reiher, B. Kirchner, J. Hutter, D. Sellmann, B. A. Hess, *Chem. Eur. J.* **2004**, *10*, 4443–4453.
[31] D. Sellmann, J. Sutter, Biological N_2 fixation: Molecular mechanism of the nitrogenase catalyzed N_2 dependent HD-formation, the N_2 fixation inhibition and the open-side FeMoco model in *Perspectives in Coordination Chemistry*, *Vol. 7* (Eds.: A. M. Trzeciak, P. Sobota, Ziolkowski), University of Wroclaw (Poland), **2000**, pp. 49–65.
[32] D. Sellmann, B. Hautsch, A. Rösler, F. W. Heinemann, *Angew. Chem.* **2001**, *113*, 1553–1558; *Angew. Chem. Int. Ed.* **2001**, *40*, 1505–1507.
[33] D. Sellmann, W. Soglowek, F. Knoch, M. Moll, *Angew. Chem.* **1989**, *101*, 1244–1245; *Angew. Chem. Int. Ed. Engl.* **1989**, *28*, 1271–1272.
[34] *CPMD*, IBM Research Division, Zürich Research Lab., MPI für Festkörperforschung, Stuttgart **1995–1999**, MPI FKF, Stuttgart/Zürich, **1995**.
[35] N. Troullier, J. L. Martins, *Phys. Rev. B* **1991**, *43*, 1993–2006.
[36] L. Kleinmann, D. M. Bylander, *Phys. Rev. Lett.* **1982**, *48*, 1425–1428.
[37] G. J. Martyna, M. E. Tuckerman, *J. Chem. Phys.* **1999**, *110*, 2810–2821.
[38] D. Sellmann, A. Hille, F. W. Heinemann, M. Moll, M. Reiher, B. A. Hess, W. Bauer, *Chem. Eur. J.* **2004**, *10*, 4214–4224.

Received: July 13, 2004
Published online: November 18, 2004

